JACS
JOURNAL OF THE AMERICAN CHEMICAL SOCIETY
Article
pubs.acs.org/JACS

From Solution to the Gas Phase: Stepwise Dehydration and Kinetic Trapping of Substance P Reveals the Origin of Peptide Conformations

Joshua A. Silveira,[†] Kyle L. Fort,[†] DoYong Kim,[†] Kelly A. Servage,[†] Nicholas A. Pierson,[‡] David E. Clemmer,[‡] and David H. Russell*[,†]

[†]Department of Chemistry, Texas A&M University, College Station, Texas 77843, United States
[‡]Department of Chemistry, Indiana University, 800 East Kirkwood Avenue, Bloomington, Indiana 47405, United States

Supporting Information

ABSTRACT: Past experimental results and molecular dynamics simulations provide evidence that, under some conditions, electrospray ionization (ESI) of biomolecules produces ions that retain elements of solution phase structures. However, there is a dearth of information regarding the question raised by Breuker and McLafferty, "for how long, under what conditions, and to what extent, can solution structure be retained without solvent?" (*Proc. Natl. Acad. Sci. U.S.A.* **2008**, *105*, 18145). Here, we use cryogenic ion mobility-mass spectrometry to experimentally probe the structural evolution of the undecapeptide substance P (SP) during the final stages of ESI. The results reveal that anhydrous SP conformers originate from evaporation of cluster ions, specifically, $[SP + 2H]^{2+}$ $(H_2O)_n$ (n = 0 to ~50) and $[SP + 3H]^{3+}$ $(H_2O)_n$ (n = 0 to ~30), and that major structural changes do not occur during the evaporative process. In the case of $[SP + 3H]^{3+}$, the results demonstrate that a compact dehydrated conformer population can be kinetically trapped on the time scale of several milliseconds, even when an extended gas phase conformation is energetically favorable.

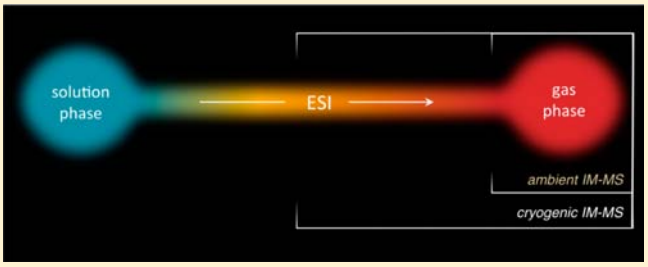

INTRODUCTION

Conformer preferences of biomolecules such as proteins and peptides are dictated by both inter- and intramolecular interactions. Because of the large number of degrees-of-freedom in bulk solvent networks and the dynamic nature of hydrogen bonds,[1−3] the specific interactions of a particular conformational state can be challenging to study in explicit environments (i.e., in solution or interacting with/inserted into a lipid membrane). Studies of solvent-free biomolecules in the gas phase provide direct information about intramolecular interactions in the absence of complicating solvation effects.[4−7] However, a potential concern is that during the transition from solution to gas phase via electrospray ionization (ESI), biomolecules encounter unique environments that can potentially affect their structures.[8−10] A number of studies have demonstrated that, upon ESI, peptide and protein ions can retain a memory of their solution structures,[11−20] suggesting that gaseous ions can be kinetically trapped in local minima along their potential energy surface owing to evaporative cooling and slow rates of isomerization. Although covalent bonds are preserved upon ESI, the effect of charge state and the extent to which noncovalent interactions (inclusive of intramolecular interactions, solvent/analyte, and adducts) are affected remain unresolved.

It is widely accepted that ESI begins with the production of charged droplets that undergo a series of evaporation and fission events under the influence of an electric field at ambient pressure and temperature, ultimately generating ions that are depleted of bulk solvent. Several models describing the generation of gas phase ions from nanodroplets have been proposed. A growing body of literature suggests that ions such as those from folded proteins are generated by the charge residue model (CRM) originally described by Dole and coworkers,[21,22] whereby small nanodroplets containing a single analyte species evaporate to yield dry ions that can retain native structure in the gas phase. Recent molecular dynamics simulations by Breuker and McLafferty suggest that during the final stages of evaporation, remnant solvent adducts surround the outermost charged residues thereby shielding intramolecular interactions in the partially solvated protein ion.[8] Alternatively, low molecular weight species are thought to be transferred into the gas phase by the ion evaporation model (IEM).[23] Originally proposed by Iribarne and Thompson, the IEM suggests that before charged droplets become sufficiently small such that they contain only a single solute molecule, the surface charge density is sufficient to eject an ion residing near the nanodroplet surface into the gas phase.[24] Consta and Malevanets[25] and Konermann et al.[26,27] have proposed that unfolded/extended macromolecules are ionized via a similar

Received: May 7, 2013
Published: December 6, 2013

dx.doi.org/10.1021/ja4114193 | J. Am. Chem. Soc. 2013, 135, 19147−19153

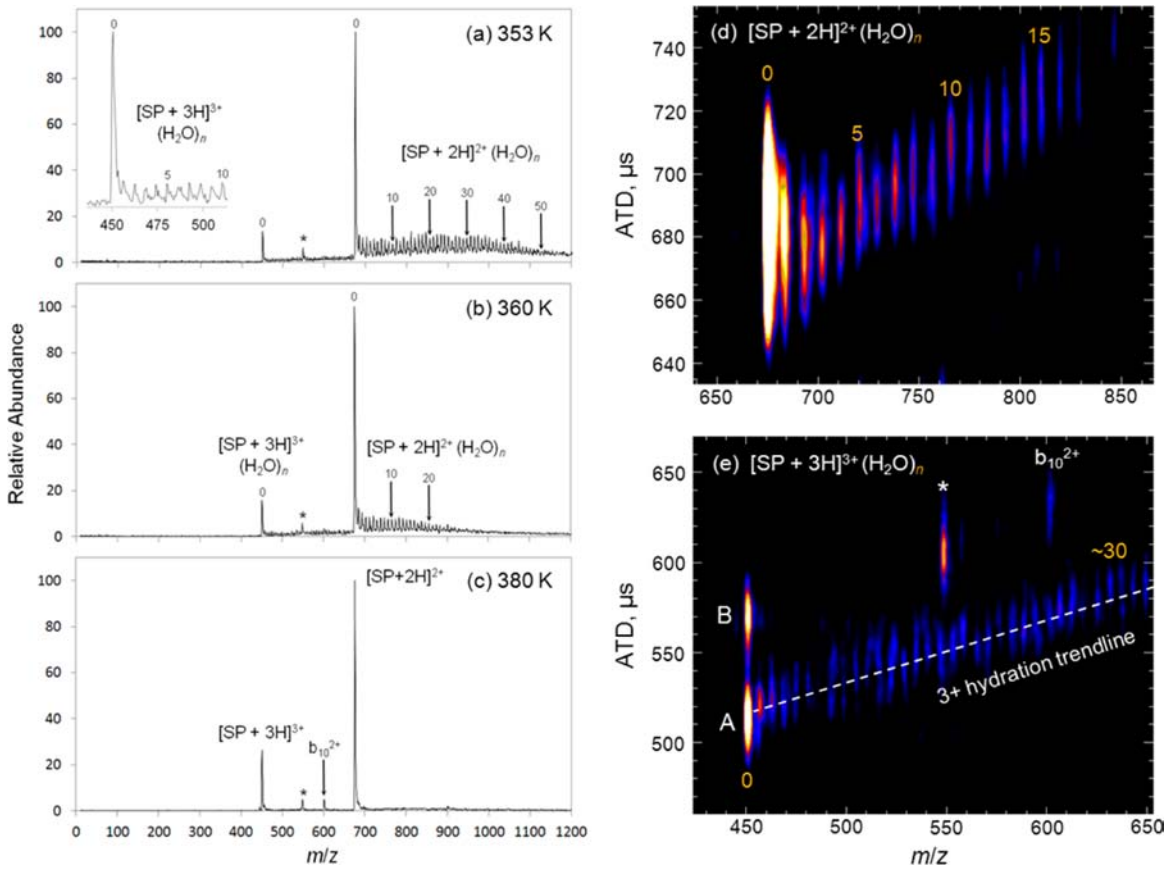

Figure 1. ESI mass spectra of SP ions captured prior to (a and b) and after (c) complete dehydration. The inset of spectrum (a) contains an expanded view of the region surrounding $[SP + 3H]^{3+}$ $(H_2O)_n$ (n = 0−10). The peak labeled with an asterisk is a contaminant ion. Two dimensional ATD versus m/z contour plots for $[SP + 2H]^{2+}$ $(H_2O)_n$ (n = 0 to ∼15) (d) and $[SP + 3H]^{3+}$ $(H_2O)_n$ (n = 0 to ∼30) (e) collected at an inlet temperature of 356 K. The trendline produced from triply charged SP hydrates is shown with a dashed line to guide the eye. $[SP + 3H]^{3+}$ conformer assignments are denoted A and B. In each experiment, the drift tube temperature was kept constant (80 ± 2 K) at a field strength of E/N 4.7 Td.

chain ejection mechanism. However, experimental techniques that can directly probe the structure and dynamics of biomolecules at intermediate extents of hydration are limited, and little is known about the final stages of desolvation during ESI. Consequently, the question posed above, "for how long, under what conditions, and to what extent, can solution structure be retained without solvent?", remains unresolved.[8]

We recently introduced cryogenic ion mobility-mass spectrometry (IM-MS) as a new technique for studying conformations of hydrated gas phase ions produced during the evaporative ESI process.[28] Here, we report a benchmark cryogenic IM-MS study that experimentally captures the evaporative dynamics of an amphipathic undecapeptide, substance P (SP, RPKPQQFFGLM-NH_2), containing both arginine and lysine residues. Previous findings suggested that water networks formed upon evaporation are largely dependent upon the particular charge-carrying species present.[28−30] Specifically, hydrated peptide ions that contain lysine and ornithine (ammonium ions) display "magic number" clusters that possess enhanced stability, whereas hydrated peptide ions that contain arginine (guanidinium ions) do not exhibit specific solvation behavior.[28] The work presented below shows that it is possible to preserve a range of peptide hydration states and directly follow structures as the naked ion emerges from solution. We find that the anhydrous SP structures are present upon evaporation of the final solvent molecules, and under some conditions, undergo transitions to other states once formed. It appears that all of a more extended state arises only after complete desolvation, and thus must be associated with a solvent-free transition.

EXPERIMENTAL METHODS

Sample Preparation. SP (95% purity, Sigma Aldrich) and SP Mutant (82% purity RPKPAAFFGLM-NH_2, MoCell Biotech Co.) were purchased and used without further purification. Peptide solutions were prepared at concentrations between 10 and 50 μM in water (18 MΩ, Barnstead, Easypure II) containing 10% methanol and 1% acetic acid. For hydration studies, SP was electrosprayed from pure water containing 0.1% formic acid.

IM-MS Measurements. The cryogenic IM-MS instrumentation and experimental details have been recently described.[28] Briefly, hydrated ions were generated by ESI and analyzed on a home-built cryogenic IM-MS apparatus. The extent of hydration was controlled using a variable temperature heated capillary inlet operated between 353 and 380 K. Cold cluster ions formed in the source region were transported into a 30.2 cm long drift tube filled with 1.6 Torr helium (T = 80 ± 2 K). Ion transport through the drift tube was facilitated by a weak electric field (9.1 V·cm^{-1}). The eluting cluster ions were pulsed into an orthogonal reflectron time-of-flight mass spectrometer for mass-to-charge (m/z) identification.

Collisional activation studies of SP were performed on a 1.38 m long home-built IM-MS instrument that operates at ambient temperature.[31] Ion activation was carried out in an ion funnel operated between 11 and 43 V cm^{-1} $Torr^{-1}$. The resulting ion populations were gated into a high-resolution periodic focusing drift tube for mobility dispersion. Determination of collision cross section

dx.doi.org/10.1021/ja4114193 | J. Am. Chem. Soc. 2013, 135, 19147−19153

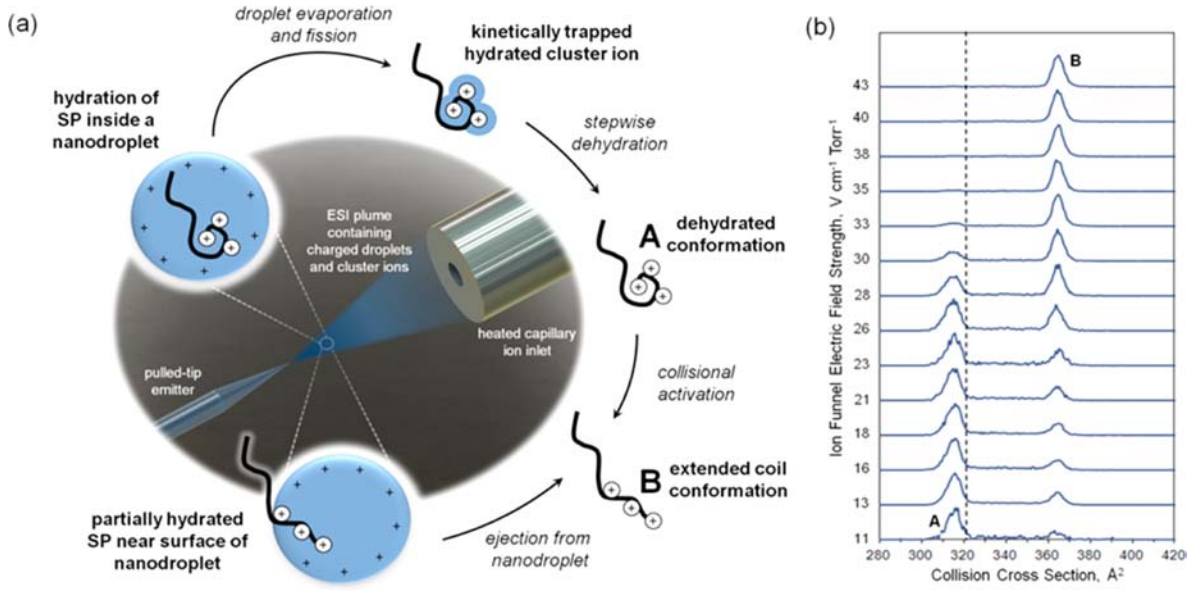

Figure 2. Two potential pathways for dehydration of $[SP + 3H]^{3+}$ ions from bulk solution via ESI: (a) The CRM (top route) describes the production of gas phase ions by evaporation of solvent from $[SP + 3H]^{3+}$ following successive fission of larger droplets. The IEM (bottom route), favored for surface-active molecules, produces ions by a field desorption process. In both cases, charged nanodroplets containing SP are produced in the ESI plume decay to ultimately yield solvent-free gas phase ions. (b) Mass-selected collision cross section profiles for $[SP + 3H]^{3+}$ ions obtained using a range of field strengths in an ion funnel prior to IM analysis. Each panel shows a separate profile where the effective ion temperature is increased by collisional activation with the helium buffer gas. For reference, the theoretical random coil trendline (321 Å^2) is shown with a dashed line. The theoretical collision cross section for $[M + 3H]^{3+}$ peptide ions was generated from a tryptic digest of a 10 component protein mixture.[54]

values in a periodic focusing electric field has been previously described.[32] Ion-helium collision cross sections were also measured using a high-resolution uniform field IM-MS instrument,[33] and there is excellent agreement (values agree to within 2% error) between the two data sets.

Molecular Dynamic Simulations. AMBER 11 and GAUSSIAN 03 were used for molecular dynamics (MD) and quantum mechanics simulations. GAUSSIAN 03 (HF/6-31+) was used to optimize the structure of custom residues and charge fitting was performed using the R.E.D. III program.[34] The AMBER FF99SB force field was used for common residues. Protons were placed on the N-terminus, the guanidine group of arginine, and the ε-amino group of lysine to model the triply charged species. MD simulations were carried out at temperatures between 300 and 550 K. Candidate structures were also generated via multiple simulated annealing runs that involved heating the system to 1000 K and slowly cooling down to 300 K over a total time of 5 ns. Clustering statistical analysis was performed on the simulated annealing structures as previously described.[35] Collision cross sections of the simulated structures were calculated using the MOBCAL software package.[36]

RESULTS AND DISCUSSION

ESI mass spectra of SP obtained from aqueous solution show abundant distributions of both $[SP + 2H]^{2+}$ $(H_2O)_n$ (n = 0 to ~50) and $[SP + 3H]^{3+}$ $(H_2O)_n$ (n = 0 to ~30) ions (see Figure 1a–c); Beauchamp et al. termed the products of this process "freeze-dried biomolecules".[30] Increasing the temperature of the ion inlet facilitates more rapid desolvation and shifts the overall distribution toward smaller cluster sizes, ultimately yielding dehydrated doubly and triply charged SP ions. Note that singly charged ions are not detected in appreciable abundance. These data not only demonstrate a high degree of control over the range of cluster size, but also show that the hydrated cluster ions detected are indeed the intermediates formed during the final stages of ESI.

The relative abundance of a particular hydrated ion is directly related to the stability of the local hydrogen bond network within the cluster.[3,28,37−39] Figure 1a–c shows that during the evaporative process, magic number clusters are not evident among the relatively smooth distributions of $[SP + 2H]^{2+}$ $(H_2O)_n$ and $[SP + 3H]^{3+}$ $(H_2O)_n$ ions. En route to forming solvent-free ions, the primary sites of water association are the charged functional groups.[8,40] While magic number clusters (n = 8, 11, 14, 20, and 40) have been previously observed for peptides and model compounds (alkyl amines), guanidinium-containing peptides are not known to display specific solvation.[7,28,30,41] Here, we hypothesize that because both functional groups are present in SP (R^1 and K^3), nonspecific water clustering likely results from interplay between the charge sites localized near the flexible N-terminus.[42]

To gain insight into the structural evolution of SP as a function of cluster size, cryogenic ion mobility was employed under inlet conditions that produce extensively hydrated ions. The data, shown in Figure 1d and e, reveal that both the doubly and triply charged ion forms of SP are comprised of dehydrated conformers that originated from evaporation of extensively hydrated ions (for $[SP + 3H]^{3+}$, this population is denoted A). The near-linear decrease in arrival time for successive n to n-1 cluster ions within each distribution reflects the small decrease in the overall collision cross section upon stepwise desolvation, suggesting that these dehydrated populations contain conformations that largely resemble their solvated counterparts. Consistent with evaporative studies by Beauchamp et al., we find no evidence for dissociation of small clusters from these hydrated peptide ions, indicating that water evaporation occurs via sequential loss of monomers.[30] Moreover, the b_{10}^{2+} fragment ion does not show evidence for water adduction, indicating that they are produced after complete desolvation. Interestingly, $[SP + 3H]^{3+}$ ions contain a second population (denoted B) observed at longer drift times that do not result

dx.doi.org/10.1021/ja4114193 | J. Am. Chem. Soc. 2013, 135, 19147−19153

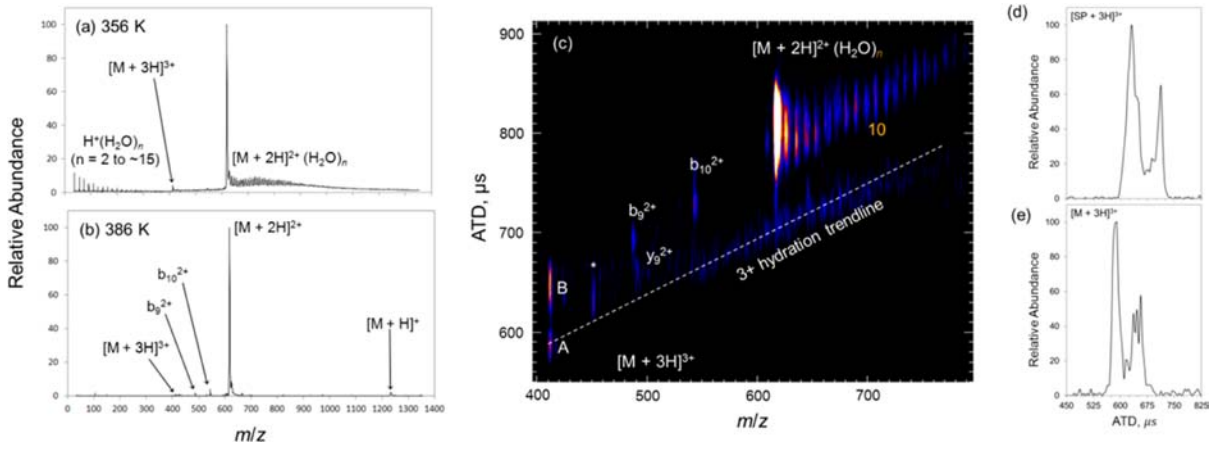

Figure 3. ESI mass spectra of mutant SP ions captured prior to (a) and after (b) complete dehydration. (c) Two dimensional ATD versus m/z contour plot for $[M + 2H]^{2+}$ $(H_2O)_n$ (n = 0 to ~15) and $[M + 3H]^{3+}$ collected at an inlet temperature of 356 K. The peak labeled with an asterisk is a contaminant ion. The extracted arrival time distribution of $[SP + 3H]^{3+}$ (d) and $[M + 3H]^{3+}$ (e) are shown for comparison.

from the evaporative process, as suggested by the absence of a dehydration trendline leading to this population. As shown in Figure 2a, there are two possible scenarios to explain this outcome: (1) conformer B is formed by the IEM, that is, expulsion from an intact nanodroplet thereby leaving no trace of its origin, or (2) B originates from a conformational change of a fully dehydrated conformer contained in population A.

Because the former hypothesis is difficult to unambiguously examine by experiment, we instead tested the latter hypothesis by collisionally heating the nascent population of ions produced upon ESI prior to ambient temperature IM-MS analysis. The results, shown in Figure 2b, confirm that populations A and B are indeed present at ambient temperature. These data support the latter hypothesis as the depopulation of A (318 Å^2) coincides with the subsequent elongation to B (368 Å^2). Note that the experimental collision cross section (CCS) values are in general agreement with previous studies (see the Supporting Information).[32,43,44] Collectively, these evaporative dynamics clearly indicate that SP ions are produced by the CRM. Hence, the transition from bulk solution to the gas phase for SP is described by the following scheme:

$$[SP + 3H]^{3+}(aq.) \xrightarrow{droplet\ evaporation\ and\ fission} [SP + 3H]_A^{3+}\,(H_2O)_{n\lesssim 30}$$

$$\xrightarrow{stepwise\ dehydration} [SP + 3H]_A^{3+} \xrightarrow{activation} [SP + 3H]_B^{3+} \xrightarrow{activation} fragments$$

The presence of multiple conformations is consistent with earlier NMR studies that showed that SP adopts helical conformations in low-dielectric environments, that is, embedded in a lipid membrane and docked in the receptor active site.[42,45] In addition, previous mass spectrometry data were interpreted as evidence for the existence of multiple conformations.[46,47] Our initial hypothesis is that the compact conformers contained within A are the result of hydrogen bonding between R^1/K^3 and Q^5/Q^6 and/or possible π-cation interactions involving F^7/F^8,[7,46−48] and that these interactions are likely responsible for kinetic trapping on the time scale of several milliseconds. The hypothesis was tested experimentally by using a mutant SP (M, RPKPAAFFGLM-NH_2) where Q^5 and Q^6 are replaced by alanine to eliminate these residues as possible hydrogen bonding sites. While replacement by alanine, valine, leucine or isoleucine would be expected to give the same effect of eliminating possible hydrogen bonding interactions, alanine was chosen because it introduces minimal steric effects.

ESI mass spectra of mutant SP ions were captured prior to (Figure 3a) and after (Figure 3b) complete dehydration. Although the hydration behavior for mutant SP $[M + 2H]^{2+}$ ions is very similar to that for SP, this is not the case for the $[M + 3H]^{3+}$ ions. The abundance of the mutant SP $[M + 3H]^{3+}$ ions and the hydrated $[M + 3H]^{3+}$ ions are appreciably lower when compared to SP. Despite the low ion yields, signals corresponding to dehydrated A and B conformers and hydrated ions of conformer A are observed (Figure 3c); however, the low abundances of the hydrated ions limit our abilities to reliably examine the effects of hydration on the collision cross sections. Moreover, the peak width for fully dehydrated A conformer of the mutant SP is narrower than that for native SP. This suggests that the conformational heterogeneity of the ion population decreased upon removing Q^5 and Q^6 (shown in Figure 3d, e) even though the relative abundances of the conformers remained unchanged. Collectively, the experimental data support the hypothesis that Q^5/Q^6 play significant roles in the stabilization of kinetically trapped populations within conformer A.

Interestingly, the presence of Q^5/Q^6 also appears to be critical to the production of the triply charged species. Charge states observed in ESI mass spectra are related to the numbers of basic residues present in the peptide;[49] however, close proximity of the charge sites can lead to a reduced charge state envelope owing to Coulombic repulsion.[50] Recently, Tsybin and co-workers have shown that the average charge state distribution of SP is increased from 2.4 to 2.8 for solutions containing 1% sulfolane.[51] Although SP adduct ions of sulfolane were observed, the sulfolane molecules were removed by mild collisional activation, which suggests that sulfolane (a good hydrogen bond acceptor) solvates the charge sites thereby mitigating the effects of Coulombic repulsion.[52] Here, it appears that intramolecular solvation of charge sites by Q^5/Q^6 stabilizes the three localized charges of the $[SP + 3H]^{3+}$ ions analogous to sulfolane, and mild collisional activation disrupts these interactions and leads to conversion of the compact conformer A to the elongated conformer B. Substitution of alanine for Q^5/Q^6 eliminates the charge solvating interactions, thereby increasing the total Coulombic repulsion within the molecule, which alters the local structure of the surrounding solvent shell and decreases the stability of the $[M + 3H]^{3+}$ ions.

dx.doi.org/10.1021/ja4114193 | J. Am. Chem. Soc. 2013, 135, 19147−19153

MD simulations yield conformations that are consistent with charge solvation of the ε-ammonium ions of K^3 by Q^5/Q^6 (Figure 4). The conformers were generated at temperatures of

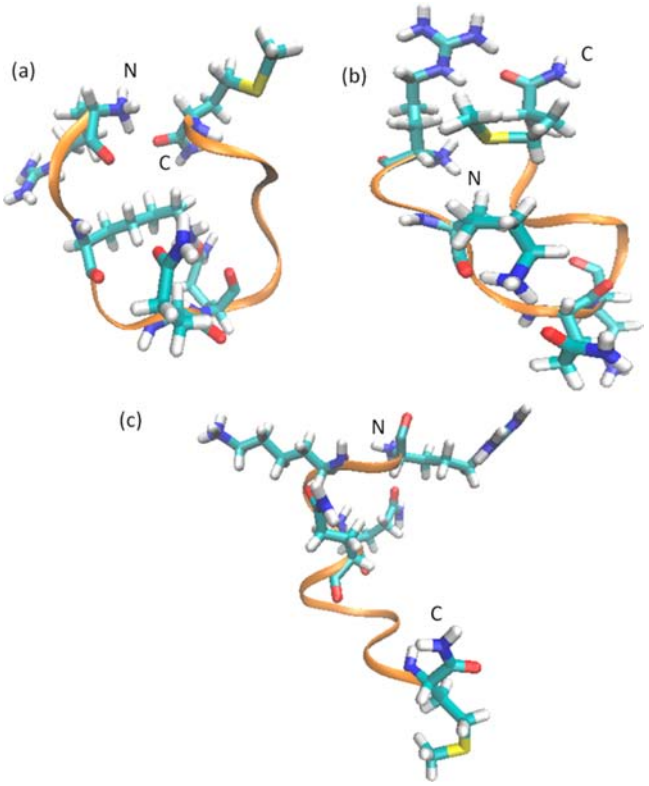

Figure 4. Representative conformers obtained via molecular dynamic simulations at (a) 300 K and (b) 550 K are shown and the representative conformer obtained by simulated annealing (c) with 300 K to 1000 K cycles. Collision cross sections for each conformer are (a) 320 Å^2, (b) 340 Å^2, and (c) 370 Å^2. As an aid to viewing the interacting side chains and the peptide backbone, several different projections of these conformations are provided in the Supporting Information.

(a) 300 K and (b) 550 K; a simulated annealing temperature cycle of 300−1000 K (see Experimental Methods) was used to generate higher energy conformations shown in (c). In addition to hydrogen bond interactions between K^3 and Q^5/Q^6, the simulations reveal significant interactions between the ammonium ion of the N-terminus and the amide C-terminus (Figure 4a). There is also evidence for hydrogen bond interactions between the guanidinium ion of R^1 and the C-terminal amide group; however, there is a paucity of conformers that have the guanidinium ion interacting with Q^5 and/or Q^6. In fact, the simulations reveal numerous conformations that display a preference of the guanidinium group to interact with the amide oxygen atoms of the peptide backbone. The absence of interactions of guanidinium ions with Q^5/Q^6, and the apparent preference for interactions with the peptide backbone amide groups is likely related to the bulky, diffuse charge and known constraints for the guanidinium ion hydrogen bond interactions. Specifically, Jungwirth showed that the guanidinium ion acts as a hydrogen bond donor along its edge, whereas the faces are poor hydrogen bond acceptors.[53]

The conformer shown in (Figure 4a) is compact (random coil) owing to intramolecular interactions involving ε-ammonium group of K^3 and the side chain amide groups of Q^5 and Q^6, as well as interactions involving the N-terminal ammonium ion and the amide group of the C-terminus. With increased temperature (Figure 4b), these interactions are disrupted and the peptide undergoes elongation. However, it should be noted that the overall conformation remains compact owing to the interaction between the guanidinium ion and the C-terminal amide group being present at 550 K. The differences between the conformations at 300 and 550 K appear to be related to projection of the guanidinium ion in (a) as opposed to being tightly bound with the C-terminal amide group through hydrogen bonds in (b). Regardless, the CCS for both conformers falls within the range of 320−340 Å^2. The lower value (320 Å^2) is in excellent agreement with the experimental CCS of A (differing by <1%), and it is reasonable to attribute the larger value (340 Å^2, which is ∼8% larger) to temperature-dependent structural changes. The conformer shown in Figure 4c is best described as an extended coil; note that intramolecular interactions involving K^3 with Q^5 and Q^6 are eliminated. The backbone appears to be helical and in fact the dihedral angles of this conformer are consistent with a helical conformation.[42,45] The agreement between MD simulations and experimental CCS provides a high level of confidence for assigning these conformations to conformers A and B (vide supra).

CONCLUSIONS

Hydrated SP ions, sampled during the final stages of the evaporative ESI process, were analyzed by cryogenic IM-MS. The results provide direct evidence that upon ESI, $[SP + 2H]^{2+}$ $(H_2O)_n$ (n = 0 to ∼50) and $[SP + 3H]^{3+}$ $(H_2O)_n$ (n = 0 to ∼30) each produce dehydrated conformers originating from stepwise evaporation of extensively hydrated clusters. Evidence for structural changes as a function of variable extents of hydration was not observed in this size range, indicating that the population of entirely dehydrated conformers resembles that of the hydrated species. IM-MS dehydration trendlines proved useful in assigning the origin of populations observed in the gas phase, especially in the case of $[SP + 3H]^{3+}$ ions that contain a second conformer (B) that does not result from the evaporative ESI process. Collisional activation of the nascent population of conformers produced upon ESI confirms that B originates from gas phase rearrangement of a conformation contained within population A. These results unambiguously show that, upon ESI, doubly and triply charged SP conformers observed in the gas phase are generated by the CRM. The ability to follow the evolution of conformers as ions emerge from differing amounts of solvent in a one-solvent-molecule-at-a-time fashion provides a powerful new approach for understanding how key elements of structure are established in a range of environments.

In the case of $[SP + 3H]^{3+}$ ions, evaporative cooling (freeze-drying) upon ESI kinetically traps a compact population of conformations (A) for several milliseconds, even though an extended conformation (B) is energetically favorable in the gas phase. In the final stages of dehydration, the stabilization afforded by solute−solvent interactions is replaced by stabilization from intramolecular interactions, that is, formation of salt-bridges and hydrogen bonding between K^3 and Q^5/Q^6. Upon removing Q^5/Q^6, these interactions no longer stabilize the $[M + 3H]^{3+}$ species. Specifically, the conformational heterogeneity of population A is reduced by the absence of these interactions. Furthermore, MD simulations indicate that the compact ion conformation is stabilized by hydrogen

dx.doi.org/10.1021/ja4114193 | J. Am. Chem. Soc. 2013, 135, 19147−19153

bonding between K^3 and Q^5/Q^6 as well as interactions between the N-terminus and C-terminus. Consistent with the low-energy collisional activation results, variable temperature MD simulations show that, upon heating, these interactions are disrupted and result in an elongation of the conformation. Furthermore, upon eliminating these interactions, the ion yield of the $[SP + 3H]^{3+}$ species is diminished. Collectively, these data illustrate that intramolecular solvation plays a critical role in stabilizing ion conformations as well as the ESI charge state distribution.

■ ASSOCIATED CONTENT

Supporting Information

Different projections of $[SP + 3H]^{3+}$ confirmations contained in Figure 4. This material is available free of charge via the Internet at http://pubs.acs.org.

■ AUTHOR INFORMATION

Corresponding Author

russell@mail.chem.tamu.edu

Notes

The authors declare no competing financial interest.

■ ACKNOWLEDGMENTS

The funding for the design, construction, and development of the cryo-IM-MS instrument was provided by the National Science Foundation-Major Research Instrument Development Program (DBI-0821700). The Department of Energy, Division of Chemical Sciences (BES DE-FG02-04ER15520) provided funding for the studies of ion hydration described herein. Funding for simulations was provided by National Science Foundation (Grant No. CHE-0541587). We wish to acknowledge Dr. Lisa Perez and the Laboratory for Molecular Simulations for many helpful discussions regarding MD simulations.

■ REFERENCES

(1) de Grotthuss, C. J. T. *Ann. Chim.* **1806**, *LVIII*, 54.
(2) Marx, D.; Tuckerman, M. E.; Hutter, J.; Parrinello, M. *Nature* **1999**, *397*, 601.
(3) Shin, J.-W.; Hammer, N. I.; Diken, E. G.; Johnson, M. A.; Walters, R. S.; Jaeger, T. D.; Duncan, M. A.; Christie, R. A.; Jordan, K. D. *Science* **2004**, *304*, 1137.
(4) Prell, J. S.; Chang, T. M.; O'Brien, J. T.; Williams, E. R. *J. Am. Chem. Soc.* **2010**, *132*, 7811.
(5) Prell, J. S.; Correra, T. C.; Chang, T. M.; Biles, J. A.; Williams, E. R. *J. Am. Chem. Soc.* **2010**, *132*, 14733.
(6) Garand, E.; Kamrath, M. Z.; Jordan, P. A.; Wolk, A. B.; Leavitt, C. M.; McCoy, A. B.; Miller, S. J.; Johnson, M. A. *Science* **2012**, *335*, 694.
(7) Nagornova, N. S.; Rizzo, T. R.; Boyarkin, O. V. *Science* **2012**, *336*, 320.
(8) Breuker, K.; McLafferty, F. W. *Proc. Natl. Acad. Sci. U.S.A.* **2008**, *105*, 18145.
(9) Skinner, O.; McLafferty, F.; Breuker, K. *J. Am. Soc. Mass Spectrom.* **2012**, *23*, 1011.
(10) Hall, Z.; Robinson, C. *J. Am. Soc. Mass Spectrom.* **2012**, *23*, 1161.
(11) Pierson, N. A.; Valentine, S. J.; Clemmer, D. E. *J. Phys. Chem. B* **2010**, *114*, 7777.
(12) Heuvel, R. H. H. v. d.; Heck, A. J. R. *Curr. Opin. Chem. Biol.* **2004**, *8*, 519.
(13) Ruotolo, B. T.; Giles, K.; Campuzano, I.; Sandercock, A. M.; Bateman, R. H.; Robinson, C. V. *Science* **2005**, *310*, 1658.
(14) Barrera, N. P.; Di Bartolo, N.; Booth, P. J.; Robinson, C. V. *Science* **2008**, *321*, 243.
(15) Pierson, N. A.; Chen, L.; Valentine, S. J.; Russell, D. H.; Clemmer, D. E. *J. Am. Chem. Soc.* **2011**, *133*, 13810.
(16) van der Spoel, D.; Marklund, E. G.; Larsson, D. S. D.; Caleman, C. *Macromol. Biosci.* **2011**, *11*, 50.
(17) Breuker, K.; Brüschweiler, S.; Tollinger, M. *Angew. Chem., Int. Ed.* **2011**, *50*, 873.
(18) Wyttenbach, T.; Bowers, M. T. *J. Phys. Chem. B* **2011**, *115*, 12266.
(19) Papadopoulos, G.; Svendsen, A.; Boyarkin, O.; Rizzo, T. *J. Am. Soc. Mass Spectrom.* **2012**, *23*, 1173.
(20) Deng, Z.; Thontasen, N.; Malinowski, N.; Rinke, G.; Harnau, L.; Rauschenbach, S.; Kern, K. *Nano Lett.* **2012**, *12*, 2452.
(21) Dole, M.; Mack, M. M.; Hines, R. L.; Mobley, R. C.; Ferguson, L. D.; Alice, M. B. *J. Chem. Phys.* **1968**, *49*, 2240.
(22) Mack, L. L.; Kralik, P.; Rheude, A.; Dole, M. *J. Chem. Phys.* **1970**, *52*, 4977.
(23) Nguyen, S.; Fenn, J. B. *Proc. Natl. Acad. Sci. U.S.A.* **2007**, *104*, 1111.
(24) Iribarne, J. V.; Thompson, B. A. *J. Chem. Phys.* **1976**, *64*, 2287.
(25) Consta, S.; Malevanets, A. *Phys. Rev. Lett.* **2012**, *109*, 148301.
(26) Konermann, L.; Ahadi, E.; Rodriguez, A. D.; Vahidi, S. *Anal. Chem.* **2012**, *85*, 2.
(27) Ahadi, E.; Konermann, L. *J. Am. Chem. Soc.* **2011**, *133*, 9354.
(28) Silveira, J. A.; Servage, K. A.; Gamage, C. M.; Russell, D. H. *J. Phys. Chem. A* **2013**, *117*, 953.
(29) Chang, T. M.; Cooper, R. J.; Williams, E. R. *J. Am. Chem. Soc.* **2013**, *135*, 14821.
(30) Lee, S.-W.; Freivogel, P.; Schindler, T.; Beauchamp, J. L. *J. Am. Chem. Soc.* **1998**, *120*, 11758.
(31) Fort, K. L.; Silveira, J. A.; Russell, D. H. *Anal. Chem.* **2013**, *85*, 9543.
(32) Silveira, J. A.; Jeon, J.; Gamage, C. M.; Pai, P.-J.; Fort, K. L.; Russell, D. H. *Anal. Chem.* **2012**, *84*, 2818.
(33) Koeniger, S. L.; Merenbloom, S. I.; Valentine, S. J.; Jarrold, M. F.; Udseth, H. R.; Smith, R. D.; Clemmer, D. E. *Anal. Chem.* **2006**, *78*, 4161.
(34) Dupradeau, F.-Y.; Pigache, A.; Zaffran, T.; Savineau, C.; Lelong, R.; Grivel, N.; Lelong, D.; Rosanski, W.; Cieplak, P. *Phys. Chem. Chem. Phys.* **2010**, *12*, 7821.
(35) Chen, L.; Shao, Q.; Gao, Y.-Q.; Russell, D. H. *J. Phys. Chem. A* **2011**, *115*, 4427.
(36) Jarold, M. F. http://www.indiana.edu/~nano/software.html (October 10, 2013).
(37) Searcy, J. Q.; Fenn, J. B. *J. Chem. Phys.* **1974**, *61*, 5282.
(38) Shi, Z.; Ford, J. V.; Wei, S.; Castleman, A. W. *J. Chem. Phys.* **1993**, *1993*, 8009.
(39) Miyazaki, M.; Fujii, A.; Ebata, T.; Mikami, N. *Science* **2004**, *304*, 1134.
(40) Wyttenbach, T.; Liu, D.; Bowers, M. T. *Int. J. Mass Spectrom.* **2005**, *240*, 221.
(41) Rodriguez-Cruz, S. E.; Klassen, J. S.; Williams, E. R. *J. Am. Soc. Mass Spectrom.* **1997**, *8*, 565.
(42) Augé, S.; Bersch, B.; Tropis, M.; Milon, A. *Biopolymers* **2000**, *54*, 297.
(43) Koeniger, S. L.; Merenbloom, S. I.; Sevugarajan, S.; Clemmer, D. E. *J. Am. Chem. Soc.* **2006**, *128*, 11713.
(44) Pierson, N. A.; Chen, L.; Russell, D. H.; Clemmer, D. E. *J. Am. Chem. Soc.* **2013**, *135*, 3186.
(45) Gayen, A.; Goswami, S. K.; Mukhopadhyay, C. *Biochim. Biophys. Acta* **2011**, *1808*, 127.
(46) Mihalca, R.; Kleinnijenhuis, A.; McDonnell, L.; Heck, A. R.; Heeren, R. A. *J. Am. Soc. Mass Spectrom.* **2004**, *15*, 1869.
(47) Gill, A. C.; Jennings, K. R.; Wyttenbach, T.; Bowers, M. T. *Int. J. Mass Spectrom.* **2000**, *195–196*, 685.
(48) Addario, V.; Guo, Y.; Chu, I. K.; Ling, Y.; Ruggerio, G.; Rodriquez, C. F.; Hopkinson, A. C.; Siu, K. W. M. *Int. J. Mass Spectrom.* **2002**, *219*, 101.
(49) Covey, T. R.; Bonner, R. F.; Shushan, B. I.; Henion, J.; Boyd, R. K. *Rapid Commun. Mass Spectrom.* **1988**, *2*, 249.

(50) Schnier, P. D.; Gross, D. S.; Williams, E. R. *J. Am. Soc. Mass Spectrom.* **1995**, *6*, 1086.
(51) Miladinovic, S. M.; Fornelli, L.; Lu, Y.; Piech, K. M.; Girault, H. H.; Tsybin, Y. O. *Anal. Chem.* **2012**, *84*, 4647.
(52) Douglass, K. A.; Venter, A. R. *J. Am. Soc. Mass Spectrom.* **2012**, *23*, 489.
(53) Wernersson, E.; Heyda, J.; Vazdar, M.; Lund, M.; Mason, P. E.; Jungwirth, P. *J. Phys. Chem. B* **2011**, *115*, 12521.
(54) McLean, J. A.; Ruotolo, B. T.; Gillig, K. J.; Russell, D. H. *Int. J. Mass Spectrom.* **2005**, *240*, 301.